20th Australasian Fluid Mechanics Conference
Perth, Australia
5-8 December 2016

Simulation and Experimental Validation of an Axial-Flow Hydrocyclone

O. A Oakman[1, 2] and J. L. Liow[1]

[1] School of Engineering and Information Technology
UNSW, Canberra, Northcott Drive, Canberra, ACT, 2600, Australia

[2]Capability Acquisition and Sustainment Group
Department of Defence, Russell Offices, ACT 2610, Australia

Abstract

An axial-flow hydrocyclone separator is a potentially viable alternative to the conventional reverse-flow hydrocyclone that currently dominate the chemical and metallurgical industries. The straight through flow design lends itself to lower pressure losses and, in turn, reduce energy consumption. A numerical model of a cylindrical axial-flow miniature hydrocyclone with a diameter of 5 mm was developed to investigate the flow structure within the axial hydrocyclones, its separation efficiency and pressure drop characteristics. This model was compared to experimental data obtained from an identical model for validation. The pressure drop in the axial hydrocyclones was found to be lower (with Euler numbers around 100) than the corresponding conventional reverse-flow hydrocyclones which operate with Euler numbers above 1000. The onset of turbulent flow within the axial-flow hydrocyclones was found to occur at a Reynolds number much closer to that of swirling pipe flow (Re~2500) rather than the reverse-flow hydrocyclones (Re~1000). The turbulent flow was modelled with a large eddy simulation model. The numerical modelling indicated that the use of a tangential feed inlet leads to asymmetry in the flow field and also creates recirculating vortices in the centre of the hydrocyclone. This in turn leads to a strong recirculation at the base of the hydrocyclone and particularly at the vortex finder outlet. A preliminary investigation into separation showed that due to the recirculation at the hydrocyclone base, this axial-flow hydrocyclone did not perform well. The results indicate that these devices could be a viable alternative to reverse-flow hydrocyclones but there is still scope for further careful design to minimize mixing and ensure that the particles are not recirculated back to the central core leading to reduced separation efficiencies.

Introduction

The hydrocyclone is a common separation device for solid-liquid and liquid-liquid separation in the chemical and mineral industry [7]. Hydrocyclones with a diameter smaller than 10 mm have been designated mini-hydrocyclones to distinguish them from those with diameters larger than 10 mm which is the minimum size commonly used commercially [9]. Most of the hydrocyclones used in industry utilise the reverse-flow configuration in which the lighter fraction, comprising of the finer solids, exit the hydrocyclone at the top is called the overflow. The heavier fraction, comprising of the coarser solids, exit through the base is called the underflow. The use of axial, uniflow or through-flow hydrocyclones is not common, although they have been used for heavy media separation in the coal industry. Axial cyclones for solid-gas separation have been studied for high temperature separation of solids from fluid catalytic cracking (FCC) gases [1] and for exhaust gas purification [6]. As both the products exit at the same end of the hydrocyclone, a major design constraint has been the management of the concentric outlet flow.

Although the use of the reverse-flow hydrocyclone has been entrenched in industry, the axial-flow hydrocyclone can offer certain advantages. First, without the reverse-flow, entrainment due to mixing during flow reversal is minimised. Second, studies have shown that axial-flow hydrocyclones have a lower pressure drop per unit length of the separation unit [6] compared to reverse-flow hydrocyclones. Third, the manufacture of an axial-flow hydrocyclone body is simpler with micro-machining techniques than for a reverse-flow hydrocyclone since a conical body with a small angle is not essential. The design of the axial-flow hydrocyclone is governed by the inlet and outlets. For the inlet, the uniflow type cyclones tend to have the feed stream in parallel with the hydrocyclone cylinder and vanes or swirlers are needed to impart a rotation to the flow. The use of a tangential inlet similar to those used for the reverse-flow hydrocyclones is more advantageous as it removes the difficulty in manufacturing, maintaining and installing the vanes and swirlers, particularly if the hydrocyclone has a small diameter.

In this study, an axial-flow mini-hydrocyclone is investigated to determine the design parameters that affect the flow and separation efficiency to provide some guidelines on how best to improve the performance of axial-flow hydrocyclones. A tangential feed entry is used to introduce the swirl as this simplifies the manufacturing of the axial-flow mini-hydrocyclone.

Experimental Method

An axial-flow mini-hydrocyclone with a cylindrical internal diameter of 5 mm was studied to determine its separation efficiencies and pressure drops with different inlet velocities. A schematic of the hydrocyclone is shown in Figure 1. The hydrocyclone is constructed with Perspex and held together with 3 mm diameter bolts that are used to align the separate sections, each of which is machined separately on a micro-milling machine [5]. A pressure transducer was connected through a T-piece close to the feed inlet and the two outlet streams were diverted to separate collection bins for analysis.

The feed stream consisted of 0.5 wt% (0.2 vol%) of solid spherical soda lime glass particles ($\rho_{particle}$=2520 kg/m^3) which was introduced using two different pumps. For the lower flow rates, a volumetric flask of 1800mL was placed on the magnetic stirrer and the particle-laden fluid was pumped through the ISMATEC MCP-Z Standard magnetic pump to provide a pulseless flow. For higher flow rates, the feed was directly injected from a pressurised chamber filled with the particle-laden fluid into the hydrocyclone. The exit streams were collected separately into a one litre beaker for the underflow outlet and a

300mL beaker for the vortex finder (termed overflow here to allow comparison with the reverse-flow hydrocyclone) outlet based on the anticipated volumetric split of the exit streams. The particle size distribution of the feed was analysed with a Malvern Mastersizer 2000 particle size analyser (PSA) is shown in Figure 2. The particle size distribution shows a bimodal distribution with an average particle size of 25 micrometres. For each run, pressure readings were taken three times over the period of the run and the volumetric split between the outlets was recorded. The outlet streams were initially weighed, and a sample removed for particle size analysis. The rest of the water was then evaporated slowly so that the amount of particles collected could be weighed. Microscopic analysis of the particles indicated that there was minimal breakage during the measurement process.

Dimension	Size (mm)
Cylinder diameter (D)	5.0 [D]
Feed inlet ($a \times b$)	1.33 × 1.67 [4/15D × D/3]
Length (L)	10.0 [2D]
Vortex finder diameter (c)	0.83 [D/6]
Vortex finder length (V_L)	1.6 [D/3]
Vortex finder wall thickness	0.5 [D/10]
Underflow outlet ($a' \times b'$)	1.33 × 3.33 [4/15D × 2D/3]

Table 1. Dimensions of the axial hydrocyclone.

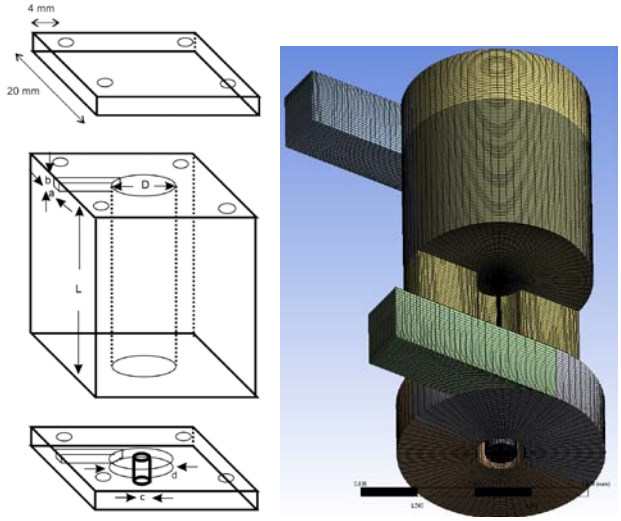

Figure 1. Left: Schematic of the Perspex model of the axial-flow hydrocyclone. Right: The computational mesh for the axial-flow hydrocyclone.

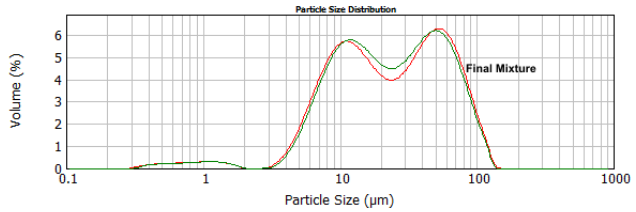

Figure 2. Particle size distribution of the soda lime spherical glass spheres used as the solid for the feed stream.

Numerical Method

The performance of the axial hydrocyclone was modelled using the Fluent v14.5 package in double precision similar to the method used by Zhu *et al.* [9]. Wherever possible, a structured Cartesian mesh was used. The skewed cells at the interface between the tangential inlet and outlet and the unstructured elements throughout the centre of the cyclone did not cause any numerical instability during computational runs. Tests with runs up to 3.8 million grid cells showed that grid independence was achieved with 1.02 million grid cells. Subsequently, the rest of the runs were conducted with 1.02 million grid cells. The Pressure Staggered Option (PRESTO) scheme was used for the pressure gradient approximation, which is suitable for the large gradients expected in swirling flows. The gradients were resolved using the Least Squares Cell Based algorithm. The Bounded Central Differencing scheme was used to resolve the momentum terms and reduce non-physical oscillation which is required when using the Smagorinsky-Lilly LES model due to its low numerical diffusion. A Bounded Second Order Implicit scheme was used for the time stepping. The Pressure-Implicit with Splitting of Operators (PISO) algorithm was used for the coupling of pressure and velocity.

The inlet velocity was used as the inlet boundary condition and the atmospheric pressure was used as the pressure condition for the outlets. The flow profile at the inlet was obtained from a steady state velocity profile where a 500 mm length of the same rectangular channel was simulated to obtain the steady state flow profile. Water properties at 20°C was used to define the inlet fluid properties and for the cases where particles were introduced into the flow, inert, spherical particles with a diameter range 1×10^{-6} m $\leq Dp \leq 1\times10^{-4}$ m were defined where the experimental particle size distribution was fitted to a Rosin-Rammler-logarithmic distribution. The properties of the soda-lime spherical particles used in the experiment were used for these particles. The convergence condition was set to the residuals being $\leq 10^{-5}$. The simulations were run for to give approximately 2.3 residence times in the hydrocyclone. Pressure averages and mass flow rates at the inlet and both outlets, and the velocity components at the centroid of the hydrocyclone were tracked with time.

Experimental Results

Pressure Drop

The pressure drop across the hydrocyclone was measured for a range of flowrates and is shown in Figure 3. The pressure drop data was correlated with the Euler and Reynolds numbers defined as

$$Eu = \frac{2\Delta P}{\rho_c v_{ch}^2},$$

$$Re = \frac{v_{ch} D}{\nu}.$$

where ρ_c and ν are the density and kinematic viscosity of the water respectively, D is the cyclone diameter, and $v_{ch}=4Q/(\pi D^2)$ is the velocity in the cyclone cylinder. This definition is similar to that used by Svarosvky [7] and Vieira *et al.* [8] allowing a comparison of the pressure drop characteristics with reverse-flow hydrocyclones.

At low Reynolds number, the Euler number decreases inversely with increasing Reynolds number which is similarly to the pressure drop in circular pipes in the laminar region. At high Reynolds number, the Euler number reaches an asymptote, in this case it is around an Euler number of 100. This asymptote is reached by a Reynolds number of 10^4, which suggests that the swirling flow in the axial hydrocyclone acts to dissipate momentum similar to a very rough surface. The micro-milled internal surfaces of the axial-flow hydrocyclone are smooth with roughness of the order of a few micrometres as observed under a scanning electron microscope. Hence it is likely that the dominant pressure losses are due to the flow rather than the surface roughness. The asymptote for a reverse-flow hydrocyclone has an Euler number around 1000 [7, 8]. For the same Reynolds number, the pressure drop for an axial hydrocyclone is lower than that for a reverse-flow hydrocyclone.

The Reynolds number where the Euler number begins to flatten out is around 2000 to 3000 which is similar to the region of transitional flow in a circular pipe.

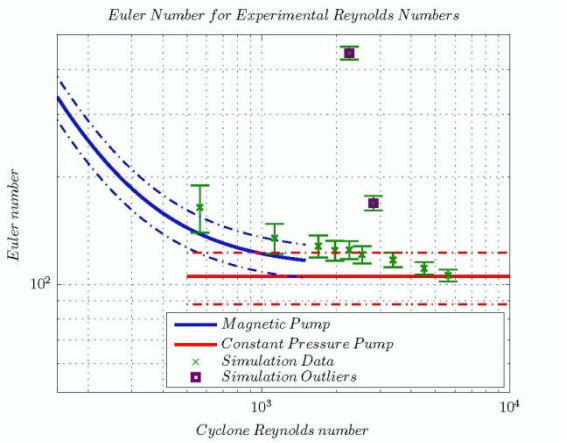

Figure 3. Dimensionless pressure drop (Euler number) as a function of flow rate represented by the Reynolds number for the experimental and numerical results.

Volumetric Split Ratio

The volumetric split ratio of the flows for the axial-flow hydrocyclone is shown in Figure 4 and it is fairly independent of the Reynolds number. The volumetric split ratio is fairly large compared to other hydrocyclones that have been studied mainly due to the fact that the ratio of the underflow to overflow exit area for this axial hydrocyclone is 7.3 while it is usually much less for most hydrocyclones. The ratio of inlet to outlet flow area is 0.56 and hence the velocity is reduced by half as it approaches the exit. This, in turn, affected the separation efficiency.

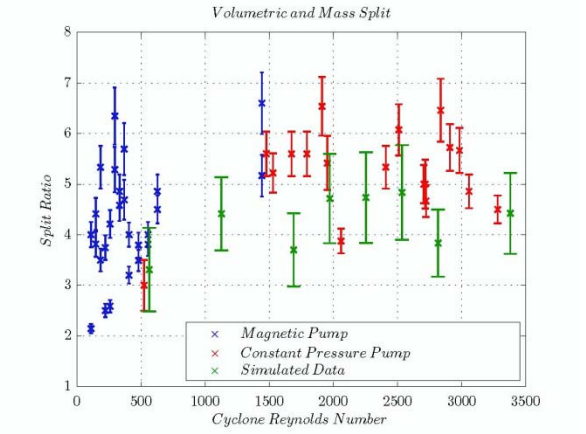

Figure 4. Split ratio of volume to underflow to volume to overflow. The value stays roughly constant across the Reynolds number range studied.

Separation Efficiencies

The separation efficiencies for this design was found to be quite poor and the highest inlet velocity that could be reached was 2.6 m/s with the magnetic pump and 6.0 m/s with the constant pressure pump. The numerical simulation was used to understand the flow field in the hydrocyclone to determine what caused the poor separation efficiency.

Numerical Results

The numerical simulation studied a range of velocities as listed in Table 2. The simulations were carried out for 2.3 times average residence time of the feed and Figure 5 shows that the averaged mass flow rates through the exits have settled to a value close to the long term average. The flows through the exits are unsteady but the variation with time is small after two times the average residence time. A large proportion of the flow exits through the underflow and only a small fraction through the central vortex finder. This is in agreement with the experimental split ratio as shown in Figure 4. The pressure drops predicted are in good agreement with the experimental measurements as shown in Figure 3. Two points showed a quite different pressure drop as they fell in the transition region between laminar and turbulent where the pressure fluctuations varied significantly with time. Further detailed simulations will be required in this region to ascertain what role the flow instabilities present in the transition region affect the numerical simulations.

Inlet velocity, m/s	*Re*	Swirl No. (at *H*=0.5)	Average residence time (ms)
1.0	564	23.9	124
2.0	1127	21.6	62
3.0	1691	17.3	41
4.0	2255	19.4	31
5.0	2818	13.3	25
6.0	3382	11.8	21
8.0	4510	10.9	15
10.0	5637	9.2	12

Table 2. List of simulations.

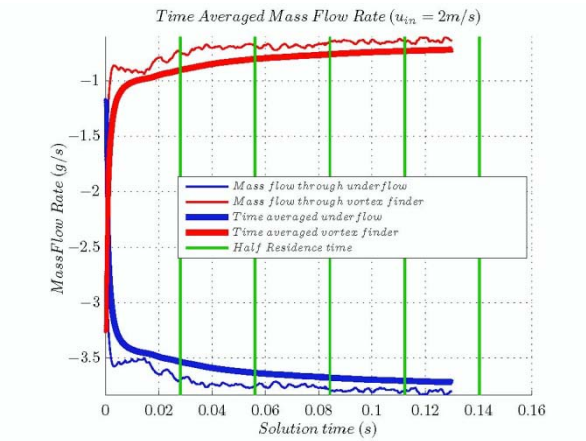

Figure 5. Flow rate as a function of simulation time for the exit streams for the axial-flow hydrocyclone showing a rapid convergence to the average flow rate for an inlet velocity of 5 m/s.

The separation efficiencies were found to be quite low at low velocities and improved minimally with the higher velocities. However the separation efficiencies were not high for all the runs. This is potentially related to the design of the hydrocyclone which had a much larger exit area compared to the inlet area, to ease the manufacture of the hydrocyclone. The tangential velocity, however, had a significantly larger peak velocity which was found to be skewed to one side of the cyclone. This caused an uneven centrifugal force around the cylinder. To quantify the degree of swirling present, the swirl number representing the non-dimensional angular momentum flux was calculated at the mid-point of the hydrocyclone [3].

$$\Omega = 2\int_0^r \frac{u_\theta u_z}{R^3 u_{av}^2} dr$$

where R is the radius of the hydrocyclone, and r is the radial location. The swirl numbers for the axial-flow hydrocyclone at *0.5H* are shown in Table 2. There is a decrease in swirl number as the Reynolds number increases. The swirl numbers obtained, however, are much higher than that of reverse-flow

hydrocyclones, in which a swirl number of $\Omega \geq 4$ would be considered high-intensity swirl [2]. The large disparity is probably due to the increased tangential velocity peaks in axial-flow hydrocyclones compared to reverse-flow hydrocyclones.

The velocity flow field is shown in Figure 6 for an inlet velocity of 5 m/s. It shows the typical flow field found in the hydrocyclone. The flow fields for all the simulation from inlet velocities of 1 m/s to 10 m/s showed that the flow was asymmetric, which is expected, as the feed was introduced tangentially at one entry point on the side of the cylinder.

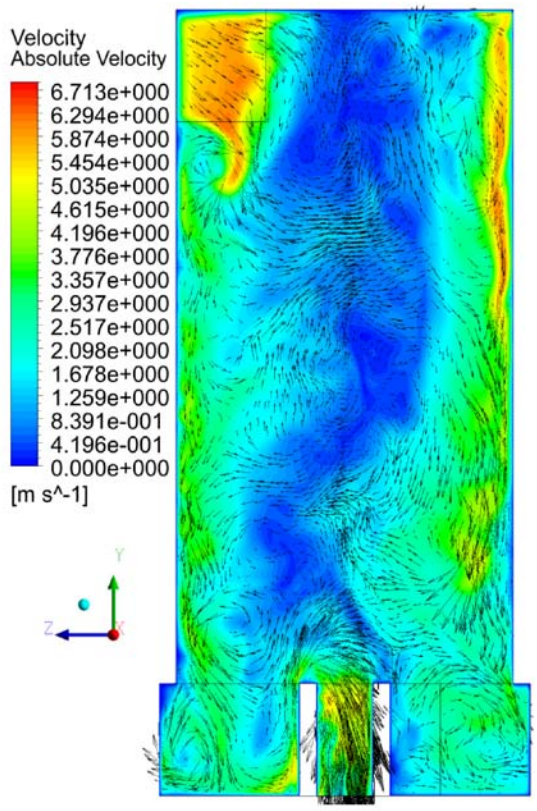

Figure 6. Velocity vectors for an inlet velocity of 5 m/s at t=0.0378 s (1.5× average residence times) from start of the simulation.

The feed stream flows along the outer section of the cylinder and there is a downward flow of the fluid down the wall of the cylinder. In the centre, vortices form resulting in recirculation of the fluid. Thus the feed stream does not flow progressively down from the feed to the exit. A vortex exists at the top of the cylinder which is similar to the recirculation zone that occurs between the feed and vortex finder in the reverse-flow hydrocyclones. This upper vortex induces subsequent vortices that extend down to the exits.

Two strong recirculating vortices seen at the base of the hydrocyclone suggest that a toroidal vortex is formed due to the presence of sharp corners present. The flow in the base region is skewed with a larger vortex present at the end opposite to the feed side and a smaller vortex on the same side as the feed. The smaller vortex only fills half the space and a counter vortex fills the other half. The counter vortex provides material that feeds into the vortex finder tube. As such, the particles exiting the overflow will not be much different to the underflow. This is reflected in the experimental results. The velocity distribution also shows that most of the high velocities occur at the outer radius of the cylinder with the centre having a lower velocity and hence, minimal separation capability. In many analyses of hydrocyclones, a solid body rotation of the fluid is assumed and the velocity should increase linearly with radial distance. In this case, the central portion up to half a radius from the centre has an absolute velocity less than 10% of the maximum velocity.

Theoretical analysis such as that of Kutepov & Lagutkin [4] assumes that the feed stream is concurrent with the hydrocyclone cylinder and hence asymmetry is assumed not to be present. The use of the tangential feed inlet is shown to lead to asymmetry of the fluid flow and this affects the separation and flow characteristics all the way down the body of the axial hydrocyclone.

Conclusions

A model of the axial-flow hydrocyclone was studied experimentally and numerically to identify the flow field and operating characteristics of axial-flow hydrocyclones so that they can be optimised to operate more efficiently. The study showed that flow asymmetry and the formation of recirculating vortices in the body of the hydrocyclone has a strong influence on the ability of the axial-flow hydrocyclone to separate particle efficiently. Based on this study, new designs to minimise the asymmetry and recirculating vortices will be developed for the axial-flow hydrocyclone.

References

[1] Gauthier, T. A., Briens, C. L. & Bergougnou, M. A. Uniflow cyclone efficiency study. *Powder Technology*, **62**, 1990, 217–225.

[2] Ko, J., Zahrai, S., Macchion, O. & Vomhoff, H. Numerical modeling of highly swirling flows in a through-flow cylindrical hydrocyclone. *AIChEJ*, **52**, 2006, 3334–3344.

[3] Kreith, F. & Sonju, O. The decay of a turbulent swirl in a pipe. *Journal of Fluid Mechanics*, **22**(2), 1965, 257–271.

[4] Kutepov, A. M. & Lagutkin, M. G. Modelling of separation in a cocurrent cylindrical hydrocyclone. *Theoretical Foundations of Chem. Engng.*, **37**(3), 2003, 230–236.

[5] Liow, J. L., Mechanical micromachining: a sustainable micro-device manufacturing approach? *Journal of Cleaner Production*, **17**, 2009, 662–667.

[6] Nieuwstadt, F. & Dirkzwager, M. A fluid mechanics model for an axial cyclone Separator. *Industrial and Chemistry Research*, **34**(10), 1995, 3399–3404.

[7] Svarovsky, L. *Hydrocyclones*. Holt, Rinehard and Winston, London, 1984.

[8] Vieira, L. G. M., Barbosa, E. A., Damasceno, J. J. R., & Barrozo, M. A. S. Performance analysis and design of filtering hydrocyclones. *Brazilian Journal of Chemical Engineering*, **22**, 2005, 143–152.

[9] Zhu, G. F., Liow, J. L. & Neely, A. Computational study of the flow characteristics and separation efficiency in a mini-hydrocyclone. *Chemical Engineering Research and Design*, **90**(12), 2012, 2135-2147.